JOURNAL OF GEOPHYSICAL RESEARCH, VOL. 111, C12007, doi:10.1029/2006JC003539, 2006

Nonlinear generation and loss of infragravity wave energy

Stephen M. Henderson,[1] R. T. Guza,[1] Steve Elgar,[2] T. H. C. Herbers,[3] and A. J. Bowen[4]

Received 10 February 2006; revised 20 July 2006; accepted 17 August 2006; published 8 December 2006.

[1] Nonlinear energy transfers with sea and swell (frequencies 0.05–0.40 Hz) were responsible for much of the generation and loss of infragravity wave energy (frequencies 0.005–0.050 Hz) observed under moderate- and low-energy conditions on a natural beach. Cases with energetic shear waves were excluded, and mean currents, a likely shear wave energy source, were neglected. Within 150 m of the shore, estimated nonlinear energy transfers to (or from) the infragravity band roughly balanced the divergence (or convergence) of the infragravity energy flux, consistent with a conservative energy equation. Addition of significant dissipation (requiring a bottom drag coefficient exceeding about 10^{-2}) degraded the energy balance.

Citation: Henderson, S. M., R. T. Guza, S. Elgar, T. H. C. Herbers, and A. J. Bowen (2006), Nonlinear generation and loss of infragravity wave energy, *J. Geophys. Res.*, *111*, C12007, doi:10.1029/2006JC003539.

1. Introduction

[2] Infragravity waves are low frequency (0.005–0.05 Hz) surface gravity waves. In the inner surf zone, where breaking limits the amplitude of higher frequency (0.05–0.40 Hz) sea and swell waves, infragravity waves sometimes contribute much of the total wave energy [*Holman and Bowen*, 1984; *Guza and Thornton*, 1985].

[3] Theory predicts that infragravity waves are generated by low-frequency modulations in the momentum flux ('radiation stress') and mass flux ('Stokes drift') of sea-swell waves [*Longuet-Higgins and Stewart*, 1962; *Hasselmann et al.*, 1963; *Symonds et al.*, 1982; *Schäffer*, 1993, 1994]. Models for infragravity wave generation predict much of the temporal and cross-shore variability of infragravity energy observed in the field [*Herbers et al.*, 1995; *Raubenheimer et al.*, 1996; *Reniers et al.*, 2002; *Van Dongeren et al.*, 2003].

[4] Statistically significant phase coupling between pairs of sea-swell waves (with frequencies f and $f + \Delta f$) and an infragravity wave (frequency Δf) has been observed in the field using bispectral analysis [*Hasselmann et al.*, 1963; *Elgar and Guza*, 1985; *Ruessink*, 1998; *Sheremet et al.*, 2002]. Such phase coupling is associated with nonlinear energy transfers between sea-swell and infragravity waves [*Herbers and Burton*, 1997]. In the laboratory, nonlinear energy transfers were calculated by *Battjes et al.* [2004] as part of a detailed energy balance. Here, the rate of nonlinear energy transfer to and from infragravity waves is calculated from phase coupling observed on a beach in North Carolina. Recent analysis by *Thomson et al.* [2006] of the infragravity energy balance on a California beach, concurrent with the analysis presented here, but using different methods, yielded similar results.

[5] A conservative, weakly nonlinear energy balance equation for infragravity waves (section 2) is combined with field observations (section 3) to calculate nonlinear energy transfer rates (section 4). Nonlinear interactions were responsible for both generating and removing infragravity energy. Under moderate- and low-energy conditions, nonlinear transfers approximately balanced gradients in the cross-shore infragravity energy flux, consistent with the conservative energy balance. Simplifications of the energy balance, and possible explanations for infragravity energy loss, are discussed in section 5. Infragravity energy losses were observed in the absence of breaking, and were not a result of frictional dissipation. Results are summarized in section 6.

2. Theory

2.1. Energy Balance

[6] A depth-integrated, conservative energy balance for statistically steady, alongshore-uniform, shallow water infragravity waves is (Appendix A)

$$\frac{\partial F(f)}{\partial x} = W(f), \tag{1}$$

where $F(f)$ is the net cross-shore energy flux at a cyclic infragravity frequency f, x is the cross-shore coordinate (positive offshore), and $W(f)$ is the nonlinear transfer of energy to motions at frequency f from motions at other frequencies. In the linear approximation [*Sheremet et al.*, 2002], $F(f)$ is the flux carried by seaward-propagating waves minus the flux carried by shoreward-propagating waves. Small amplitude sea-swell waves (amplitude/depth of order $\epsilon \ll 1$) and smaller amplitude infragravity waves (order ϵ^n, where $1 < n < 2$) are assumed, and equation (1)

[1] Scripps Institution of Oceanography, La Jolla, California, USA.
[2] Woods Hole Oceanographic Institution, Woods Hole, Massachusetts, USA.
[3] Department of Oceanography, Naval Postgraduate School, Monterey, California, USA.
[4] Department of Oceanography, Dalhousie University, Halifax, Nova Scotia, Canada.

0148-0227/06/2006JC003539$09.00

will be evaluated to order ϵ^{2+n}. Under these approximations, nonlinear transfers $W(f)$ are dominated by interactions with sea-swell waves. Rollers, and interactions between waves and mean currents, are neglected. No assumptions are made concerning wave reflection at the shoreline.

[7] The energy flux will be expressed in terms of the cross-spectral density

$$\Phi_f(X,Y) = \frac{E\left[\langle X\rangle_f \langle Y\rangle_{-f}\right]}{df} \tag{2}$$

$$= \frac{1}{2}\left[\mathcal{C}_f(X,Y) + \mathrm{i}\mathcal{Q}_f(X,Y)\right], \tag{3}$$

where $E[\cdot]$ is the expected value, X and Y are real variables, $\langle X\rangle_f$ is the frequency-f infinitesimal complex amplitude [*Priestley*, 1981] of X (similarly for $\langle Y\rangle_f$), df is the infinitesimal frequency resolution, and $\mathcal{C}$ and $\mathcal{Q}$ are one-sided co- and quad-spectral densities. For nearly shore-normal shallow water waves, the net energy flux at an infragravity frequency f is

$$F(f) = h\mathcal{C}_f(g\eta,u) + \mathcal{C}_f(g\eta,M) + \mathcal{C}_f(\mathsf{S}_{xx},u), \tag{4}$$

where

$$M = \eta' u', \quad \mathsf{S}_{xx} = hu'u' + g\eta'\eta'/2, \tag{5}$$

g is gravitational acceleration, h is the still water depth, u is the seaward velocity, η is the sea-surface elevation above the still water level, and primes ($'$) denote sea-swell variables (band-passed between 0.05 and 0.40 Hz). The slowly varying part of the sea-swell mass flux M equals the slowly varying depth-integrated Stokes drift [*Phillips*, 1977, section 3.3]. The slowly varying part of S_{xx} is a component of the sea-swell radiation stress [*Longuet-Higgins and Stewart*, 1964]. The first term on the right of (4) is the linear energy flux [*Sheremet et al.*, 2002; *Henderson and Bowen*, 2002; *Thomson et al.*, 2006] and the remaining terms are nonlinear corrections (section 5.2).

[8] For nearly shore-normal shallow water waves, the nonlinear energy transfer to motions at an infragravity frequency f,

$$W(f) = \mathcal{C}_f(\mathsf{S}_{xx}, \partial u/\partial x), \tag{6}$$

is the deformation work done by the slowly varying radiation stress on the infragravity strain rate. Positive W values indicate energy transfer to motions at frequency f, whereas negative values indicate transfer from motions at frequency f. Equation (6) resembles formulas for the turbulent production rate, in which the Reynolds stress takes the part of the radiation stress [*Tennekes and Lumley*, 1972]. *Phillips* [1977] and *Schäffer* [1993] derived fully nonlinear equations for interactions between waves and slowly varying mean flows, which can be applied to infragravity waves if infragravity frequencies are assumed much lower than sea-swell frequencies. Equations (1), (4), and (6) require no such assumptions regarding wave frequencies, but are weakly nonlinear and assume nearly shore-normal propagation. When all assumptions are satisfied (when infragravity waves are weakly nonlinear, relatively low frequency, and nearly shore-normal), the equations of *Phillips* [1977] and *Schäffer* [1993] are equivalent to (1), (4), and (6).

2.2. Triad Interactions

[9] The nonlinear energy transfers described by (6) result from wave triad interactions. The total energy transfer to frequency f is (Appendix B)

$$W(f) = \int_{f_1\in\mathcal{I}} w(f_1, f-f_1)\, df_1, \tag{7}$$

where $w(f_1, f-f_1)$ is the energy transfer to (or from) an infragravity frequency f by a triad of waves with frequencies f, f_1, and $f-f_1$, and $\mathcal{I}$ is the set of f_1 values for which f_1 and $f-f_1$ are both sea-swell frequencies (triads for which f_1 and $f-f_1$ are not both sea-swell frequencies are negligible under the scaling of section 2.1). In terms of the cross-bispectral density [*Priestley*, 1981]

$$\Phi_{f_1,f_2}(X,Y,Z) = \frac{E\left[\langle X\rangle_{f_1}\langle Y\rangle_{f_2}\langle Z\rangle_{-f_1-f_2}\right]}{df_1\, df_2} \tag{8}$$

$$= \frac{1}{2}\left[\mathcal{C}_{f_1,f_2}(X,Y,Z) + \mathrm{i}\mathcal{Q}_{f_1,f_2}(X,Y,Z)\right], \tag{9}$$

(here $\mathcal{C}_{f1,f2}(X,Y,Z)$ and $\mathcal{Q}_{f1,f2}(X,Y,Z)$ are one-sided co- and quad-bispectral densities), the energy transfer by a triad is

$$w(f_1,\, f-f_1) = h\,\mathcal{C}_{f_1,f-f_1}(u,u,\partial u/\partial x) + \frac{g}{2}\,\mathcal{C}_{f_1,f-f_1}(\eta,\eta,\partial u/\partial x). \tag{10}$$

[10] Equations (6), and (7)–(10), are equivalent expressions for $W(f)$ (Appendix B). A pair of sea-swell waves with frequencies f_1 and $f-f_1$ produces a frequency-f fluctuation in the radiation stress. The total radiation stress fluctuation at frequency f is produced by many such pairs of sea-swell waves, each with a different value of f_1. The work done by the frequency-f radiation stress fluctuation from a single pair of waves is $w(f_1, f-f_1)$, and the total work done by the radiation stress, $W(f)$, is the integral of $w(f_1, f-f_1)$ over all values of f_1.

[11] The nonlinear transfer term of *Herbers and Burton*'s [1997] Boussinesq model can be derived as a special case of (7) and (10) (Appendix C).

3. Field Observations and Data Processing

[12] Data were collected on an ocean beach near Duck, North Carolina, during the Duck94 experiment [*Elgar et al.*, 1997]. Water pressure and velocity were measured (at 2 Hz) at 13 locations along a cross-shore transect extending from the shore to about 5-m water depth (Figure 1). Seabed elevations were estimated with surveys from an amphibious vehicle [*Lee and Birkemeier*, 1993], and with sonar altimeters collocated with pressure and current sensors.

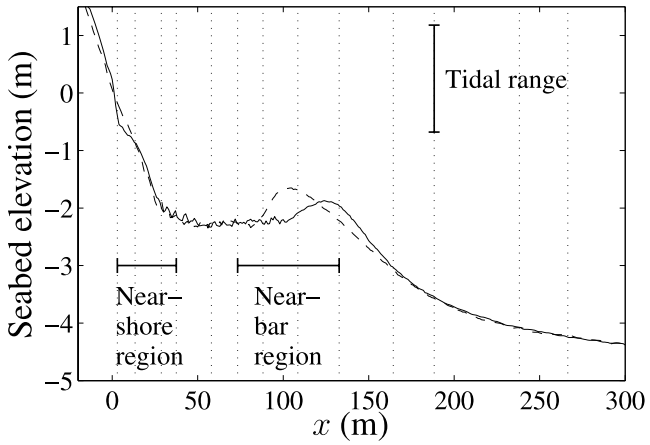

Figure 1. Seabed elevation (relative to mean sea level) versus cross-shore distance x on 7 September (solid curve) and 26 September (dashed curve). Vertical dotted lines indicate cross-shore locations of collocated pressure and velocity sensors. Regions of integrated energy balances are indicated (see text). The mean shoreline location is $x = 0$ (equivalent to $x = 131$ m in FRF coordinates).

[13] Data collected between 1 September and 11 October 1994, when the beach was relatively alongshore-uniform [*Ruessink et al.*, 2001], were analyzed. During this period, the crest of the sandbar (Figure 1) remained between 100 and 140 m offshore. To minimize departures from the alongshore-uniform balance (1), 3-hour time series at a given location were excluded when the linear alongshore energy flux (calculated from the co-spectrum between pressure and alongshore velocity) integrated over infragravity frequencies exceeded 150% of the linear cross-shore flux (for the alongshore-uniform balance to hold in such cases, the alongshore length scale over which the alongshore energy flux varies would have to be much greater than the across-shore scale over which the across-shore flux varies [*Henderson and Bowen*, 2002]).

[14] During the Duck94 experiment, shear waves often were more energetic than infragravity waves. Wave-current interactions, the likely source of shear wave energy, were omitted from the energy balance (1). Cases with energetic shear waves were excluded, with the exceptions of Figure 2 and section 5.5, discussed below. Observations at a given cross-shore location were excluded if shear wave energy (averaged over 3 hours, and calculated using the method of *Lippmann et al.* [1999]) exceeded 75% of infragravity energy at that location, or if shear wave energy (3-hour averaged) exceeded 150% of infragravity energy at any cross-shore location. These criteria do not remove all shear wave energy, but few cases would satisfy more severe criteria.

[15] Although infragravity waves can contribute much of the total wave energy near the shore (depths less than about 1 m, *Holman and Bowen* [1984], *Guza and Thornton* [1985], and many others), infragravity waves were significantly smaller than sea-swell waves in the cases considered here (the measured infragravity pressure variance never exceeded 11% of the sea-swell pressure variance).

[16] Two-Hertz time series of M and S_{xx} were calculated by substituting the measured depth, together with band-passed (0.05–0.40 Hz) pressure and velocity, into (5). Cross-spectra and bispectra were calculated by dividing 3-hour time series into 50 non-overlapping segments and Fourier transforming, giving a cross-spectral frequency resolution near 5×10^{-3} Hz. Bispectral estimates also were smoothed in the frequency-domain (section 4).

[17] To evaluate nonlinear transfers from (6) and (10), the cross-shore gradient of the cross-shore velocity must be known. Solving the shallow water mass conservation equation

$$\frac{\partial \eta}{\partial t} + \frac{\partial [(h+\eta)u]}{\partial x} = 0 \tag{11}$$

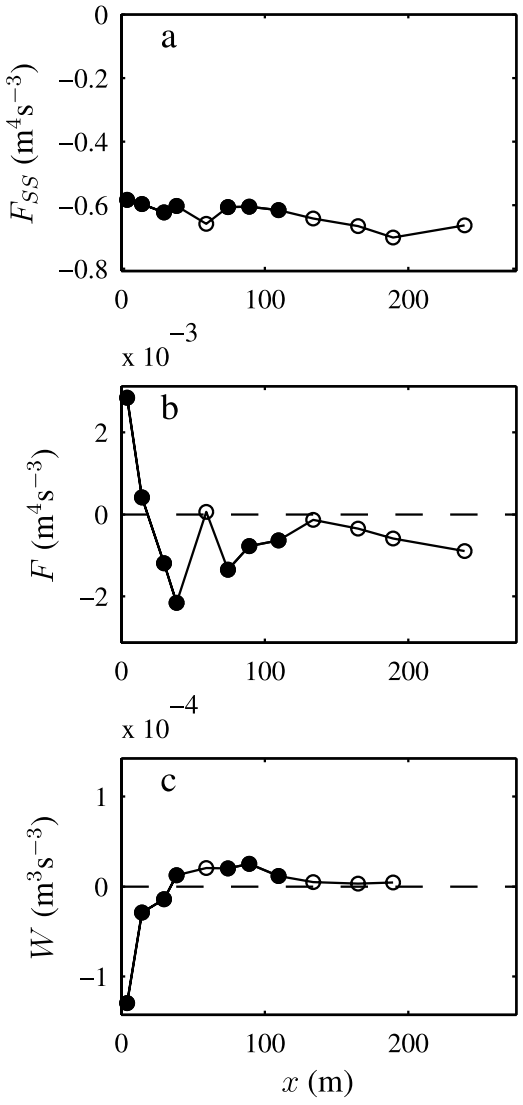

Figure 2. Energy fluxes and transfer rates versus cross-shore distance x for 7 September, 1900–2200 EST. (a) Linear energy flux at sea-swell frequencies F_{SS} (negative values indicate shoreward flux). (b) Net (seaward minus shoreward) infragravity energy flux F (13). (c) Nonlinear energy transfer to infragravity waves W (14). Open symbols indicate observations with significant shear wave contributions (section 3) excluded from subsequent analysis.

for $\partial u/\partial x$ and neglecting the wave mass flux gradient $\partial(\eta u)/\partial x$ yields

$$\frac{\partial u}{\partial x} = -\frac{1}{h}\left(\frac{\partial \eta}{\partial t} + u\frac{\partial h}{\partial x}\right). \quad (12)$$

To estimate $\partial h/\partial x$, depths at adjacent instruments were finite-differenced. Two-Hertz time series of $\partial u/\partial x$ were estimated from (12), and substituted into (6) and (10) to estimate nonlinear transfers. Neglecting the wave mass flux gradient in (12) introduces an $O(\epsilon^4)$ error in W, which is negligible under the assumed ordering (section 2). To check the accuracy of (12), $\partial u/\partial x$ also was calculated by finite-differencing velocity measurements from adjacent instruments. Resulting estimates of cross-shore integrated nonlinear transfers (W^{INT}, section 4) usually were within 10% of corresponding estimates made using (12).

4. Results

[18] On 7 September, 1900–2200 EST, sea-swell waves were small (significant wave height H_s = 0.40 m in 8-m depth), and propagated past the most shoreward sensors without breaking. Consequently, in this case the measured sea-swell energy flux F_{SS} was nearly constant (Figure 2a). In other cases, a breaking-induced shoreward decrease in F_{SS} was observed (not shown). The observed energy flux integrated over infragravity frequencies,

$$F = \int_{f=0.005\,\mathrm{Hz}}^{0.050\,\mathrm{Hz}} F(f)\,df, \quad (13)$$

diverged (increased seawards) near the bar crest (x = 74–134 m, Figure 2b, and 84% of all 3-hour time series in the data set), indicating a net infragravity energy gain, and converged near the shore (x = 4–39 m, Figure 2b, and 76% of all 3-hour time series), indicating a net infragravity energy loss.

[19] Cases of energetic shear waves are shown in Figure 2 (open circles) because, if shear wave cases are removed, cross-shore profiles become sparse. Shear wave cases (including the cases presented in Figure 2) are excluded from all results discussed in the text of this paper (as described in section 3), with the exception of section 5.5. Shear waves often were energetic in cases with large sea-swell waves, so the data presented include only cases of low and moderate sea and swell energy (significant wave heights in 8-m depth ranged from 0.3 to 1.2 m). The total nonlinear energy transfer to infragravity waves,

$$W = \int_{f=0.005\,\mathrm{Hz}}^{0.050\,\mathrm{Hz}} W(f)\,df, \quad (14)$$

often was positive near the bar, and negative near the shore (e.g., Figure 2c). Scatter of point estimates of W was reduced by calculating the integrated nonlinear transfer across a section of beach $W^{\mathrm{INT}} = \int_a^b W\,dx$ (using the trapezoidal rule between adjacent instruments). From the theoretical energy balance (1),

$$W^{\mathrm{INT}} = \Delta F, \quad (15)$$

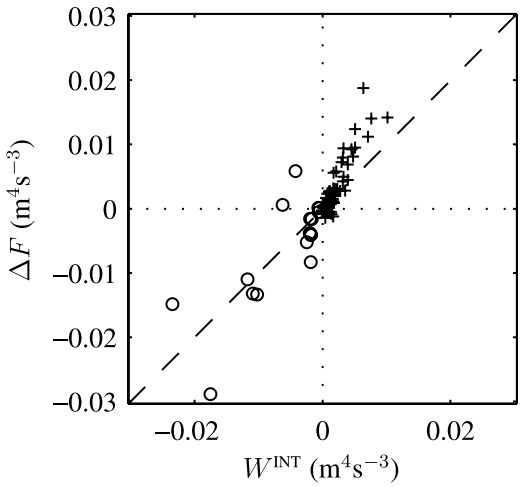

Figure 3. Change in total infragravity energy flux ΔF versus nonlinear transfer to infragravity motions W^{INT}. Pluses (circles) indicate 3-hour observations near the bar (near the shore). Dashed line indicates agreement with the conservative energy balance (15). All data (after exclusion of shear waves) are shown.

where ΔF is the change in energy flux between cross-shore locations a and b. Results were calculated for regions near the bar crest (x = 74–134 m, depth range 2.1–3.0 m, mean depth 2.5 m, Figure 1) and near the shore (x = 4–39 m, depth range 0.5–2.7 m, mean depth 1.8 m). After removing cases of shear waves and strong alongshore energy fluxes (section 3), 86 separate estimates of W^{INT} and ΔF remained.

[20] The observed ΔF and W^{INT} roughly balanced, ($\Delta F = 1.2 \times \Delta W + 7 \times 10^{-4}$ m^{4}s^{-3}, with r^2 = 0.76, Figure 3). Positive energy transfer rates W^{INT} and flux divergences ΔF were observed near the bar crest (pluses, Figure 3). Negative W^{INT} and ΔF values were observed near the shore (circles, Figure 3). Near the bar crest, ΔF often was larger than W^{INT}, perhaps owing to neglected processes (e.g., wave-current interactions, four-wave interactions, surface rollers, obliquity of infragravity waves), or instrument errors. Similar results were obtained when the limits of integration in (13) and (14) were changed to evaluate the energy balance separately for low (0.005–0.025 Hz) and high (0.025–0.05 Hz) infragravity frequency bands (Figure 4). The excess of ΔF over W^{INT} near the bar crest was most severe at low infragravity frequencies.

[21] Most nonlinear generation and loss of infragravity energy occurred through triad interactions with swell (frequencies 0.05–0.15 Hz, Figure 5). The most rapid nonlinear generation observed (near the bar crest on 27 September) resulted from triads comprising an infragravity wave and two swell waves (Figure 5a). The most rapid nonlinear energy loss (near the shore on 13 September) also resulted from triads comprising an infragravity and two swell waves (Figure 5b). The total nonlinear transfer to infragravity waves by swell is

$$W_{\mathrm{swell}} = 2\int_{f=0.005\,\mathrm{Hz}}^{0.050\,\mathrm{Hz}} \int_{f_1=0.050\,\mathrm{Hz}+f}^{0.15\,\mathrm{Hz}} w(f_1,\, f-f_1)\,df_1\,df. \quad (16)$$

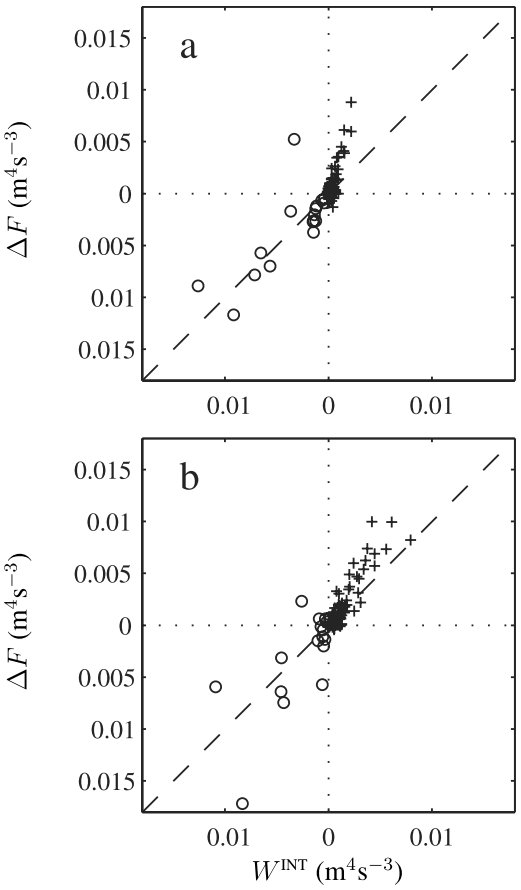

Figure 4. Change in total infragravity energy flux ΔF versus nonlinear transfer to infragravity motions W^{INT}, as Figure 3, but with energy balance evaluated separately for (a) 0.005–0.025 Hz and (b) 0.025–0.05 Hz frequency bands. Pluses (circles) indicate 3-hour observations near the bar (near the shore). Dashed line indicates agreement with the conservative energy balance (15).

For all cases of rapid nonlinear energy exchange ($|W| > 10^{-4}$ m^{4}s^{-3}), W_{swell} accounted for 72% of the total root-mean-square nonlinear transfer. Nonlinear energy transfers with infragravity waves were too small to alter the sea-swell energy balance significantly. Cross-shore integrated transfers (<0.02 m^{4}s^{-3}, Figure 3) were much less than sea-swell energy fluxes (−0.6 m^{4}s^{-3} on a day with small waves, Figure 2).

[22] Equation (6) was derived under the assumption that infragravity waves are much smaller than incident waves, and consequently neglects the triads involving two or three infragravity waves that are important to infragravity wave breaking [*Van Dongeren et al.*, 2004]. Therefore, infragravity wave breaking might invalidate the analysis. To test the importance of triads involving two or three infragravity waves, the nonlinear transfer term W defined in (6) was recalculated without excluding such triads (by replacing η' and u' in equation (5) with η and u). Differences between the two W estimates were small (considering all non-shear-wave data, $W_{IG}^{INT} = 1.2 \times W^{INT} - 2 \times 10^{-4}$ m^{4}s^{-3} with $r^2 = 0.98$, where W^{INT} is the cross-shore integrated transfer discussed above, and W_{IG}^{INT} is the corresponding transfer including multi-infragravity triads). Triads involving two or three infragravity waves might contribute to steepening or breaking of infragravity waves, but their inclusion would not change our conclusions.

5. Discussion

5.1. Dissipation

[23] Infragravity energy losses owing to bottom friction have been parameterized [e.g., *Henderson and Bowen*, 2002] as

$$D_{bed} = c_D E\left[|u|u_{IG}^2\right], \tag{17}$$

where c_D is a bottom drag coefficient and u_{IG} is the infragravity velocity. The dissipative energy balance

$$\Delta F = W^{INT} - D^{INT}, \tag{18}$$

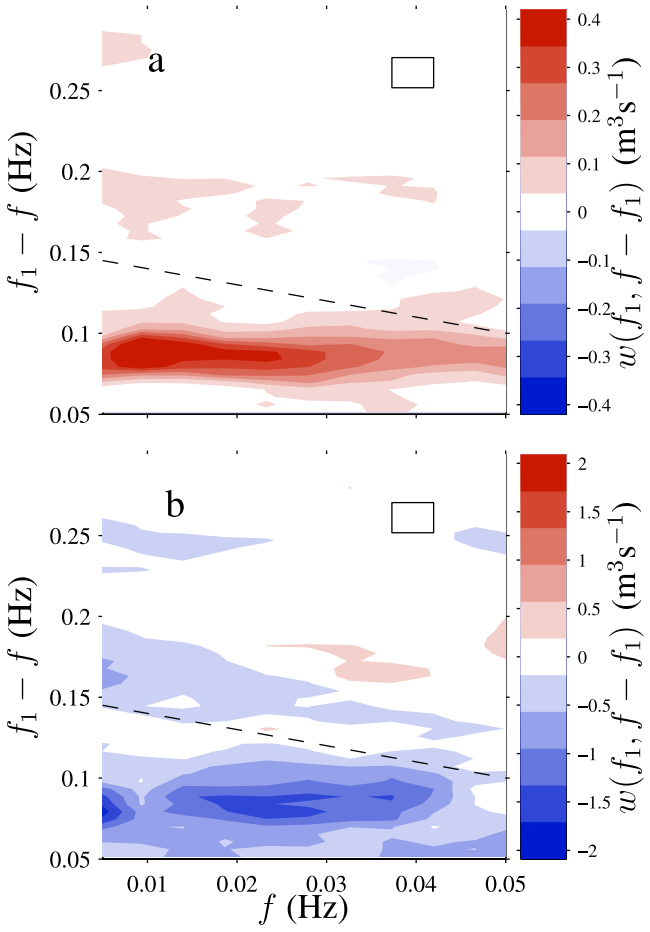

Figure 5. Nonlinear working $w(f_1, f - f_1)$ (equation (10)) on frequency f motion by triads with frequencies $(f, f_1, f - f_1)$. (a) 27 September (1000–1300), averaged between cross-shore locations (Figure 1) 90 and 110 m. (b) 13 September (1000–1300), averaged between cross-shore locations 4 and 14 m. Rectangles indicate the size of regions over which bispectra were smoothed to estimate $w(f_1, f - f_1)$. Below the dashed lines (which mark $f_1 = 0.15$ Hz), triads consist of one infragravity and two swell (0.05–0.15 Hz) waves.

evaluated over near-shore (4–39 m offshore) and near-bar (74–134 m) regions (where D^{INT} is calculated by trapezoidal integration of D_{bed}) did not fit the data better than the conservative balance (15). The best-fit c_D had a small, and nonphysical, negative value. When $c_D = 10^{-3}$ (equation (17)), the r^2 for (18) was 0.75, essentially the same as in the conservative case. When c_D was increased to 10^{-2}, r^2 declined to 0.70, and when *Henderson and Bowen*'s [2002] estimate $c_D = 0.08$ was used, r^2 declined further to 0.38.

[24] Infragravity waves are unlikely to break when the shorter, higher-energy sea-swell waves do not break. Infragravity energy losses were observed in depths for which sea-swell waves did not break (e.g., Figure 2). Therefore, breaking of infragravity waves, which might dissipate infragravity energy [*Battjes et al.*, 2004; *Van Dongeren et al.*, 2004] and lead to nonlinear energy transfers to higher frequencies [*Herbers et al.*, 2000], was not essential to the observed nonlinear energy loss. Dissipation of infragravity waves by breaking remains a possibility shoreward of the most shoreward sensor (at $x = 4$ m), and in higher-energy conditions than shown in Figure 2.

5.2. Linear Energy Flux

[25] The total energy flux

$$F = F_L + F_N, \tag{19}$$

where the linear flux

$$F_L = \int_{f=0.005\,\mathrm{Hz}}^{0.050\,\mathrm{Hz}} h\,\mathcal{C}_f(g\eta, u)\,df, \tag{20}$$

and the nonlinear flux

$$F_N = \int_{f=0.005\,\mathrm{Hz}}^{0.050\,\mathrm{Hz}} \mathcal{C}_f(g\eta, M)\,df + \int_{f=0.005\,\mathrm{Hz}}^{0.050\,\mathrm{Hz}} \mathcal{C}_f(S_{xx}, u)\,df. \tag{21}$$

The two terms on the right of (21) have similar magnitudes. The nonlinear flux F_N is assumed insignificant in many models for weakly nonlinear, nearly resonant wave interactions [*Freilich and Guza*, 1984; *Herbers and Burton*, 1997], and often is neglected so the total (F) and linear (F_L) fluxes are assumed equal [*Sheremet et al.*, 2002; *Henderson and Bowen*, 2002; *Thomson et al.*, 2006]. Near the bar ($x = 74$–134 m), the linear energy flux F_L, like the total flux F, usually diverged (87% of cases), and the divergence of F_L was correlated with, although smaller than (about 60% of), the divergence of F ($r^2 = 0.74$). However, near the shore ($x = 4$–39 m), F_L usually diverged (94% of cases), whereas F usually converged (75% of cases). Over all cases near the shore, the divergences of F_L and F were uncorrelated ($r^2 = 0.04$). Therefore, neglect of nonlinear infragravity energy fluxes was a poor approximation near the shore.

5.3. Effects of Seabed Slope

[26] The ratio between $u(\partial h/\partial x)$ and $\partial\eta/\partial t$ of (12) is of order

$$\beta = \frac{\partial h/\partial x}{kh}, \tag{22}$$

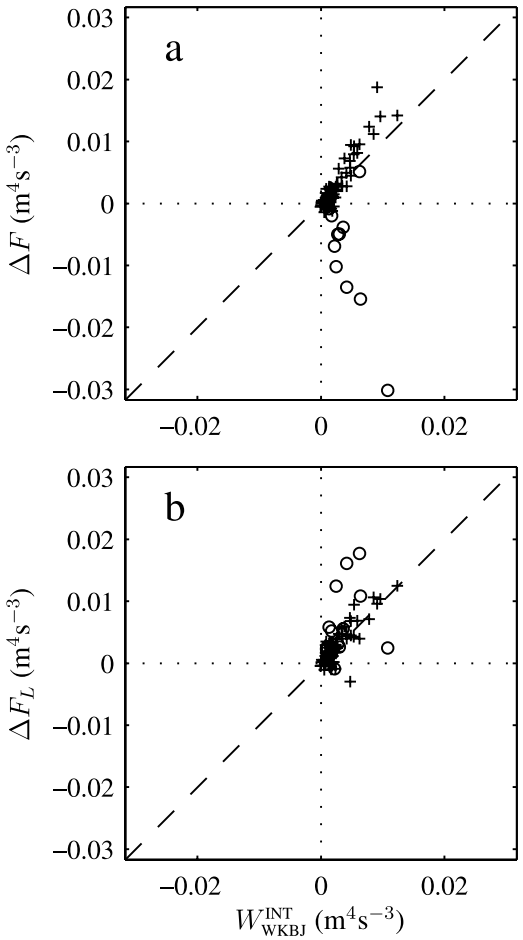

Figure 6. Change in (a) total energy flux ΔF and (b) linear energy flux ΔF_L versus nonlinear transfer to infragravity motions calculated by neglecting sloping-bed effects $W_{\mathrm{WKBJ}}{}^{\mathrm{INT}}$. Pluses (circles) indicate 3-hour observations near the bar (near the shore). Dashed line indicates agreement with the conservative energy balance (15).

where k is an infragravity radian wavenumber, and we have used the results $\partial\eta/\partial t = O(2\pi f\eta)$, $2\pi f/k = O[(gh)^{1/2}]$, and $u = O[(g/h)^{1/2}\eta]$ [*Lippmann et al.*, 1999]. Many 'WKBJ' wave models [*Longuet-Higgins and Stewart*, 1964; *Herbers and Burton*, 1997] make the small-slope approximation $\beta \ll 1$. *Battjes et al.* [2004] examined the effects of finite β on shoaling bound waves. If $\beta \ll 1$, $u(\partial h/\partial x)$ can be neglected in (12). When this term was neglected in the present data set (yielding a WKBJ estimate of nonlinear transfers denoted $W^{\mathrm{INT}}_{\mathrm{WKBJ}}$), positive nonlinear transfers over the bar were predicted well (compare pluses in Figures 6a and 3), but negative nonlinear transfers near the shore were not predicted (compare circles in Figures 6a and 3). Near the bar $\beta \approx 0.3$ (for 40 s period, $h = 2$ m, $\partial h/\partial x = 0.02$), whereas near the shore $\beta \approx 1$ (period 40 s, $h = 1$ m, and $\partial h/\partial x = 0.05$).

[27] Under the approximation $u' = -(g/h)^{1/2}\eta'$, $W^{\mathrm{INT}}_{\mathrm{WKBJ}}$ reduces to the energy transfer term of *Herbers and Burton*'s [1997] WKBJ Boussinesq model (Appendix C). Sloping-bed effects are smaller for sea and swell waves than for infragravity waves because sea and swell waves have larger wavenumbers (equation (22)). *Herbers and Burton*'s [1997]

WKBJ transfer term successfully predicts energy transfers among sea and swell waves during the Duck94 experiment, even near the shore [*Herbers et al.*, 2000].

5.4. Comparison With Models for Resonant Triads

[28] Models for weakly nonlinear, nearly resonant wave interactions [*Freilich and Guza*, 1984; *Herbers and Burton*, 1997] often neglect both nonlinear contributions to the energy flux (section 5.2) and sloping bed effects (section 5.3). These approximations lead to

$$\Delta F_L = W^{\mathrm{INT}}_{\mathrm{WKBJ}}, \tag{23}$$

where ΔF_L is the change in linear energy flux across a region, and $W^{\mathrm{INT}}_{\mathrm{WKBJ}}$ is the WKBJ approximation to total nonlinear transfer within the region. Near the bar, the linear (F_L) and total (F) flux gradients were similar (section 5.2), and errors introduced by the WKBJ approximation were small (section 5.3). Consequently, near the bar, nonlinear transfers in the WKBJ approximation roughly balanced ΔF_L, consistent with (23) (pluses, Figure 6b). Near the shore, the linear and total flux gradients often had different signs (section 5.2). This error in signs offset the failure of the WKBJ approximation to represent negative nonlinear transfers (section 5.3), so ΔF_L and $W^{\mathrm{INT}}_{\mathrm{WKBJ}}$ had the same sign (circles in Figure 6b). Therefore, although roughly consistent with the observations, (23) failed to identify nonlinear energy losses on this beach. On a different beach with a much lower slope, nonlinear energy losses were identified using (23) [*Thomson et al.*, 2006].

5.5. Shear Waves

[29] Cases with energetic shear waves (section 3) have been excluded from all results discussed above, and have been removed from all figures (with the sole exception of the open circles in Figure 2). When cases with shear waves were included, ΔF and W^{INT} were uncorrelated ($r^2 = 10^{-3}$), suggesting that processes neglected in the energy balance (15) (such as interactions with mean currents, the likely shear-wave energy source) were important.

6. Conclusions

[30] During moderate and low energy conditions, infragravity energy flux gradients roughly balanced nonlinear energy transfers to (and from) infragravity motions, indicating that nonlinear interactions with sea and swell waves were a major source (and sink) of infragravity energy. Nonlinear losses of infragravity energy occurred where infragravity waves were not breaking.

[31] With small drag coefficients ($<10^{-2}$), dissipation was too weak to affect the energy balance. With larger drag coefficients, the balance closure deteriorated. Consequently, *Henderson and Bowen*'s [2002] drag coefficient 0.08, estimated by neglecting nonlinear energy transfers, may be too high.

[32] Near a sandbar (74–134 m from shore), both non-WKBJ sloping bed effects and nonlinear contributions to the infragravity energy flux were small, as assumed in some models for nearly resonant triad interactions [*Freilich and Guza*, 1984; *Herbers and Burton*, 1997]. In contrast, closer to (4–39 m from) the shore, both sloping bed effects and nonlinear contributions to the infragravity energy flux were important to the local infragravity energy balance.

Appendix A: Energy Equation

[33] For statistically steady ($\partial E[\cdot]/\partial t = 0$) and alongshore-homogeneous ($\partial E[\cdot]/\partial y = 0$) shallow water waves [*Henderson and Bowen*, 2002, equations (11)–(13)]

$$E\Bigg[2hg\frac{\partial \Re\left\{\langle\eta\rangle_f\langle u\rangle_{-f}\right\}}{\partial x} + 2g\frac{\partial \Re\left\{\langle\eta\rangle_f\langle M\rangle_{-f}\right\}}{\partial x} + 2\Re\Bigg\{\frac{\partial\langle T_{xx}\rangle_f}{\partial x}\left\langle u+\frac{M}{h}\right\rangle_{-f} + \frac{\partial\langle T_{xy}\rangle_f}{\partial y}\left\langle u+\frac{M}{h}\right\rangle_{-f} + \frac{\partial\langle T_{xy}\rangle_f}{\partial x}\left\langle v+\frac{N}{h}\right\rangle_{-f} + \frac{\partial\langle T_{yy}\rangle_f}{\partial y}\left\langle v+\frac{N}{h}\right\rangle_{-f}\Bigg\}\Bigg] = 0, \tag{A1}$$

where, for depth-uniform flows, the momentum flux is

$$T_{xx} = (h+\eta)u^2 + g\frac{\eta^2}{2}, \tag{A2}$$

$$T_{xy} = (h+\eta)uv, \tag{A3}$$

$$T_{yy} = (h+\eta)v^2 + g\frac{\eta^2}{2}, \tag{A4}$$

$\Re\{\}$ is the real part, and the cross-shore (alongshore) wave mass flux $M = \eta u$ ($N = \eta v$).

[34] Equations (A1)–(A4) are fully nonlinear. To simplify for weakly nonlinear waves, let $\tilde{\eta}$ and η' be infragravity and sea-swell sea-surface elevation fluctuations (with typical magnitudes $\tilde{\eta}_0$ and η'_0), so that $\eta = \tilde{\eta} + \eta'$, and similarly for u. Let h_0 be a typical water depth, L be a typical horizontal scale for infragravity waves, and $\theta'_0 \ll 1$ be a typical sea-swell wave angle. Assume weak sea-swell waves and weaker infragravity waves, i.e.,

$$\epsilon = \frac{\eta'_0}{h_0} \ll 1, \tilde{\epsilon} = \frac{\tilde{\eta}_0}{h_0} = (\epsilon)^n, \tag{A5}$$

where $1 < n < 2$. In terms of the dimensionless variables

$$(x^*, y^*) = \left(\frac{x}{L}, \frac{y}{L}\right), h^* = \frac{h}{h_0}, \tag{A6}$$

$$(\tilde{\eta}^*, \eta'^*) = \left(\frac{\tilde{\eta}}{\tilde{\eta}_0}, \frac{\eta'}{\eta'_0}\right), \tag{A7}$$

$$(\tilde{u}^*, u'^*) = \left(\frac{h_0}{g}\right)^{1/2}\left(\frac{\tilde{u}}{\tilde{\eta}_0}, \frac{u'}{\eta'_0}\right), \tag{A8}$$

$$(\tilde{v}^*, v'^*) = \left(\frac{h_0}{g}\right)^{1/2}\left(\frac{\tilde{v}}{\tilde{\eta}_0}, \frac{v'}{\theta'_0\eta'_0}\right), \tag{A9}$$

$$S_{xx}{}^* = h^*u'^*u'^* + \frac{\eta'^*\eta'^*}{2}, S_{yy}{}^* = \frac{\eta'^*\eta'^*}{2}, \tag{A10}$$

$$M^* = \eta'^*u'^*, \tag{A11}$$

equations (A2)–(A4) are

$$\frac{T_{xx}}{gh_o^2} = \epsilon^2 S^*_{xx} + O(\epsilon\tilde{\epsilon}), \tag{A12}$$

$$\frac{T_{xy}}{gh_0^2} = O\left(\theta_0'\epsilon^2, \epsilon\tilde{\epsilon}\right), \tag{A13}$$

$$\frac{T_{yy}}{gh_0^2} = \epsilon^2 S^*_{yy} + O\left(\epsilon\tilde{\epsilon}, \theta_0'^2\epsilon^2\right). \tag{A14}$$

Substituting (A5)–(A14) into (A1) and retaining terms to order $\epsilon^{(2+n)}$ yields

$$E\left[2\tilde{\epsilon}^2 \frac{\partial h^* \Re\left\{\langle\eta^*\rangle_f \langle u^*\rangle_{-f}\right\}}{\partial x^*} + 2\epsilon^2\tilde{\epsilon}\frac{\partial \Re\left\{\langle\eta^*\rangle_f \langle M^*\rangle_{-f}\right\}}{\partial x^*} + 2\epsilon^2\tilde{\epsilon}\,\Re\left\{\frac{\partial \langle S^*_{xx}\rangle_f}{\partial x}\langle u^*\rangle_{-f} + \frac{\partial \langle S^*_{yy}\rangle_f}{\partial y}\langle v^*\rangle_{-f}\right\}\right] = 0. \tag{A15}$$

Returning to dimensional variables, rearranging the radiation stress terms, and using alongshore homogeneity to simplify the S_{yy} terms yields

$$\frac{\partial}{\partial x} 2\Re\left\{E\left[hg\langle\eta\rangle_f\langle u\rangle_{-f} + g\langle\eta\rangle_f\langle M\rangle_{-f} + \langle S_{xx}\rangle_f\langle u\rangle_{-f}\right]\right\} = 2\Re\left\{E\left[\langle S_{xx}\rangle_f \frac{\partial\langle u\rangle_{-f}}{\partial x} + \langle S_{yy}\rangle_f \frac{\partial\langle v\rangle_{-f}}{\partial y}\right]\right\}. \tag{A16}$$

The S_{yy} term (A16) includes an alongshore derivative, which cannot be evaluated from the cross-shore transect of instruments used here. *Lippmann et al.* [1997] found that S_{yy} was less important than S_{xx} in an idealized model of edge wave generation. The ratio between the S_{yy} and S_{xx} terms on the right of (A16) is of order $E[\tilde{v}^2]/(3E[\tilde{u}_2])$, which was less than 0.19 in all cases considered here. Neglecting S_{yy} in (A16), taking expected values, dividing by the infinitesimal frequency resolution *df*, and applying (2) and (3), yields (1).

Appendix B: Nonlinear Transfers by Wave Triads

[35] From (5) and (6),

$$W(f) = h\,\mathcal{C}_f(u'u', \partial u/\partial x) + \frac{g}{2}\mathcal{C}_f(\eta'\eta', \partial u/\partial x). \tag{B1}$$

Equations (7) and (10) follow from (B1) and the identity [*Yeh and Van Atta*, 1973; *Tugnait*, 1994]

$$\Phi_f(XY, Z) = \int_{f_1} \Phi_{f_1, f-f_1}(X, Y, Z)\, df_1, \tag{B2}$$

where $\Phi_f(XY, Z)$ is the cross-spectrum between Z and the product XY. To establish (B2), express X and Y as Fourier-Stieltjes integrals [*Priestley*, 1981]

$$X(t) = \int_{f_1=-\infty}^{\infty} e^{2\pi i f_1 t}\langle X\rangle_{f_1}, Y(t) = \int_{f_2=-\infty}^{\infty} e^{2\pi i f_2 t}\langle Y\rangle_{f_2}, \tag{B3}$$

so the product

$$X(t)Y(t) = \int_{f_1=-\infty}^{\infty}\int_{f_2=-\infty}^{\infty} e^{2\pi i (f_1+f_2)t}\langle X\rangle_{f_1}\langle Y\rangle_{f_2}. \tag{B4}$$

Substituting $f = f_1 + f_2$ into (B4) yields

$$X(t)Y(t) = \int_{f=-\infty}^{\infty}\int_{f_1=-\infty}^{\infty} e^{2\pi i f t}\langle X\rangle_{f_1}\langle Y\rangle_{f-f_1}, \tag{B5}$$

from which the frequency f complex amplitude of the product XY is

$$\langle XY\rangle_f = \int_{f_1=-\infty}^{\infty}\langle X\rangle_{f_1}\langle Y\rangle_{f-f_1}. \tag{B6}$$

Multiplying both sides of (B6) by $\langle Z\rangle_{-f}/df$ and taking the expected value yields (B2).

Appendix C: Simplification of the Nonlinear Transfer Term to the Form of *Herbers and Burton* [1997]

[36] Substituting the approximation $u' = -(g/h)^{1/2}\eta'$, and the linearized flat-bed mass conservation equation $\partial u/\partial x = -(\partial\eta/\partial t)/h$, into (6) yields

$$W(f) = -\frac{3g}{2h}\,\mathcal{C}_f\left(\eta^2, \partial\eta/\partial t\right). \tag{C1}$$

Substituting $\langle\partial\eta/\partial t\rangle_f = 2\pi i f\langle\eta\rangle_f$ into (C1) and applying (3) yields

$$W(f) = \frac{3\pi g f}{h}\,\mathcal{Q}_f\left(\eta^2, \eta\right). \tag{C2}$$

From (B2) and (C2)

$$W(f) = \frac{3\pi g f}{h}\int_{f_1}\mathcal{Q}_{f_1, f-f_1}(\eta, \eta, \eta)\, df_1. \tag{C3}$$

From (C3) and symmetry properties of the bispectrum [*Herbers and Burton*, 1997],

$$W(f) = \frac{3\pi g f}{h}\left[\int_{f_1=0}^{f}\mathcal{Q}_{f_1, f-f_1}(\eta, \eta, \eta)\, df_1 - 2\int_{f_1=0}^{\infty}\mathcal{Q}_{f_1, f}(\eta, \eta, \eta)\, df_1\right], \tag{C4}$$

which is the nonlinear transfer term of *Herbers and Burton* [1997], as renormalized by *Herbers et al.* [2000]. Reflection at frequency f is not neglected. Therefore, reflection of infragravity waves from the shore does not invalidate *Herbers and Burton*'s [1997] transfer expression.

[37] **Acknowledgments.** Funding was provided by the Office of Naval Research, the National Science Foundation, the Izaak Walton Killam Foundation, and the Natural Sciences and Engineering Research Council of Canada. Edith Gallagher, Britt Raubenheimer, the U.S. Army Corps of Engineers Field Research Facility, and the Staff of the Center for Coastal Studies made valuable contributions to obtaining the field observations.

References

Battjes, J. A., H. J. Bakkenes, T. T. Janssen, and A. R. van Dongeren (2004), Shoaling of subharmonic gravity waves, *J. Geophys. Res.*, *109*, C02009, doi:10.1029/2003JC001863.

Elgar, S., and R. T. Guza (1985), Observations of bispectra of shoaling surface gravity waves, *J. Fluid Mech.*, *161*, 425–448.

Elgar, S., R. T. Guza, B. Raubenheimer, T. H. C. Herbers, and E. L. Gallagher (1997), Spectral evolution of shoaling and breaking waves on a barred beach, *J. Geophys. Res.*, *102*, 15,797–15,805.

Freilich, M. H., and R. T. Guza (1984), Nonlinear effects on shoaling surface gravity waves, *Philos. Trans. R. Soc. London*, *A311*, 1–41.

Guza, R. T., and E. B. Thornton (1985), Observations of surf beat, *J. Geophys. Res.*, *90*, 3161–3172.

Hasselmann, K., W. Munk, and G. MacDonald (1963), Bispectra of ocean waves, in *Proceedings of the Symposium on Time Series Analysis*, *SIAM Ser. Appl. Math.*, edited by M. Rosenblatt, pp. 125–139, John Wiley, Hoboken, N. J.

Henderson, S. M., and A. J. Bowen (2002), Observations of surf beat forcing and dissipation, *J. Geophys. Res.*, *107*(C11), 3193, doi:10.1029/2000JC000498.

Herbers, T. H. C., and M. C. Burton (1997), Nonlinear shoaling of directionally spread waves on a beach, *J. Geophys. Res.*, *102*, 21,101–21,114.

Herbers, T. H. C., S. Elgar, and R. T. Guza (1995), Generation and propagation of infragravity waves, *J. Geophys. Res.*, *100*, 24,863–24,872.

Herbers, T., N. R. Russnogle, and S. Elgar (2000), Spectral energy balance of breaking waves within the surf zone, *J. Phys. Oceanogr.*, *30*, 2723–2737.

Holman, R. A., and A. J. Bowen (1984), Longshore structure of infragravity wave motions, *J. Geophys. Res.*, *89*, 6446–6452.

Lee, G., and W. Birkemeier (1993), Beach and nearshore survey data: 1985–1991, CERC field research facility, *Tech. Rep. CERC-93-3*, U.S. Army Corps of Eng., Waterw. Exp. Stn., Vicksburg, Miss.

Lippmann, T. C., R. A. Holman, and A. J. Bowen (1997), Generation of edge waves in shallow water, *J. Geophys. Res.*, *102*, 8663–8679.

Lippmann, T. C., T. H. C. Herbers, and E. B. Thornton (1999), Gravity and shear wave contributions to nearshore infragravity wave motions, *J. Phys. Oceanogr.*, *29*, 231–239.

Longuet-Higgins, M. S., and R. Stewart (1962), Radiation stress and mass transport in gravity waves, with application to 'surf beats', *J. Fluid Mech.*, *13*, 481–504.

Longuet-Higgins, M. S., and R. Stewart (1964), Radiation stresses in water waves: A physical discussion, with applications, *Deep Sea Res.*, *11*, 529–562.

Phillips, O. M. (1977), *The Dynamics of the Upper Ocean*, 2nd ed., Cambridge Univ. Press, New York.

Priestley, M. B. (1981), *Spectral Analysis and Time Series*, Elsevier, New York.

Raubenheimer, B., R. T. Guza, and S. Elgar (1996), Wave transformation across the inner surf zone, *J. Geophys. Res.*, *101*, 25,589–25,597.

Reniers, A. J. H. M., A. R. van Dongeren, J. A. Battjes, and E. B. Thornton (2002), Linear modeling of infragravity waves during Delilah, *J. Geophys. Res.*, *107*(C10), 3137, doi:10.1029/2001JC001083.

Ruessink, B. G. (1998), Bound and free infragravity waves in the nearshore zone under breaking and nonbreaking conditions, *J. Geophys. Res.*, *103*, 12,795–12,805.

Ruessink, B. G., J. R. Miles, F. Feddersen, R. T. Guza, and S. Elgar (2001), Modeling the alongshore current on barred beaches, *J. Geophys. Res.*, *106*, 22,451–22,463.

Schäffer, H. A. (1993), Infragravity waves induced by short-wave groups, *J. Fluid Mech.*, *247*, 551–588.

Schäffer, H. A. (1994), Edge waves forced by short-wave groups, *J. Fluid Mech.*, *259*, 125–148.

Sheremet, A., R. T. Guza, S. Elgar, and T. H. C. Herbers (2002), Observations of nearshore infragravity waves: Seaward and shoreward propagating components, *J. Geophys. Res.*, *107*(C8), 3095, doi:10.1029/2001JC000970.

Symonds, G., D. A. Huntley, and A. J. Bowen (1982), Two-dimensional surf beat: Long wave generation by a time-varying breakpoint, *J. Geophys. Res.*, *87*, 492–498.

Tennekes, H., and J. Lumley (1972), *A First Course in Turbulence*, MIT Press, Cambridge, Mass.

Thomson, J., S. Elgar, B. Raubenheimer, T. H. C. Herbers, and R. T. Guza (2006), Tidal modulation of infragravity waves via nonlinear energy losses in the surf zone, *Geophys. Res. Lett.*, *33*, L05601, doi:10.1029/2005GL025514.

Tugnait, J. K. (1994), Detection of non-Gaussian signals using integrated polyspectrum, *IEEE Trans. Signal Process.*, *42*, 3137–3149.

Van Dongeren, A. R., A. J. H. M. Reniers, J. A. Battjes, and I. A. Svendsen (2003), Numerical modeling of infragravity wave response during DELILAH, *J. Geophys. Res.*, *108*(C9), 3288, doi:10.1029/2002JC001332.

Van Dongeren, A. R., J. Van Noorloos, K. Steenhauer, J. A. Battjes, T. T. Janssen, and A. J. H. M. Reniers (2004), Shoaling and shoreline dissipation of subharmonic gravity waves, in *Proceedings of the 29th International Conference on Coastal Engineering*, pp. 1225–1237, Am. Soc. of Civ. Eng., Reston, Va.

Yeh, T. T., and C. W. Van Atta (1973), Spectral transfer of scalar and velocity fields in heated grid turbulence, *J. Fluid Mech.*, *58*, 233–261.

A. J. Bowen, Department of Oceanography, Dalhousie University, Halifax, NS, Canada B3H 4J1.

S. Elgar, Woods Hole Oceanographic Institution, Woods Hole, MA 02543, USA.

R. T. Guza and S. M. Henderson, Scripps Institution of Oceanography, La Jolla, CA 92093-0209, USA. (shenders@coast.ucsd.edu)

T. H. C. Herbers, Department of Oceanography, Naval Postgraduate School, Monterey, CA 93943-5122, USA.